Journal of Environmental Chemical Engineering 12 (2024) 112005

Contents lists available at ScienceDirect

Journal of Environmental Chemical Engineering

journal homepage: www.elsevier.com/locate/jece

Increasing the sustainability of copper electrorefining: Selective electrodeposition of antimony in the presence of bismuth from highly concentrated hydrochloric acid effluents

L. Hernández-Pérez, A. Muñoz-Pérez, E.M. Ortega, V. Pérez-Herranz, M.T. Montañés, M.C. Martí-Calatayud *

IEC Group, ISIRYM, Universitat Politècnica de València, Camí de Vera s/n, P.O. Box 22012, E-46071, 46022 València, Spain

ARTICLE INFO

Editor: Jose Solla-Gullon

Keywords:
Antimony
Bismuth
Selective electrodeposition
Critical raw materials
Effluent treatment
Metal recovery

ABSTRACT

Recovering critical materials from effluents of the copper electrorefining would improve the circularity and sustainability of this industry. In this task, selectivity is crucial to separate metals present in multi-component electrolytes and obtain added value products. Electrodeposition can be used to recover metals individually when their reduction takes place at different potentials. Moreover, the preferential deposition of a specific element can also be modulated under galvanostatic control. In this study, the recovery and separation of antimony and bismuth from highly concentrated hydrochloric acid solutions is investigated by means of voltammetry and electrodeposition. In potentiostatic mode, the preferential deposition of antimony takes place at − 0.25 $V_{Ag/AgCl}$, although a moderate selectivity is achieved. Under galvanostatic mode, at current densities below the limiting value (i_L), the deposition of bismuth is almost prevented, and the selectivity factor for antimony reaches the highest values. These results prove the feasibility of a highly selective antimony recovery by electrodeposition. When the i_L is exceeded, the selectivity towards antimony drops because more cathodic potentials are reached, which activate the deposition of bismuth and hydrogen evolution, thus decreasing the overall electrodeposition current efficiency. Upon an increase in the proportion of bismuth in the mixtures, high current densities also favor the deposition of this metal but decrease the contribution of hydrogen evolution reaction as compared to solutions with a higher proportion of antimony. Thus, the process can also be conducted at high electrodeposition current densities, yet at the cost of obtaining the product in the form of an alloy.

1. Introduction

The copper processing industry involves multiple separation and purification steps, starting from the ore extraction until reaching a high purity copper as the final product. Such steps impact the environment because they involve an intensive consumption of chemicals and energy, and also the release of pollutants [1,2]. During the manufacturing process, several wastes are generated, such as slag, flue dust and liquid effluents, which mostly contain copper and other metals considered impurities, including antimony, bismuth, arsenic or iron [3,4]. Some of these impurities have been classified as critical materials due to their scarcity and relevance to the economy [5]. This is the case of antimony and bismuth, which are included in the List of Critical Raw Materials of the European Commission [6] and in the List of Critical Minerals published by the U. S Geological Survey [7]. The relevance of antimony is based on its applications, among them, the most widespread is as flame retardant in several products, followed by its use in the form of alloys in liquid metal batteries [8,9]. In addition, the use of bismuth-antimony cathodes in liquid metal batteries has been studied with promising results [10]. Other applications of Sb are as glass decolorizer, catalyst in the production of plastics and semiconductor dopant [3]. Thus, recovering metals from the copper processing residues contributes to increase the sustainability of this industry.

Electrorefining is the last stage of copper production, where high-purity copper cathodes are obtained. Apart from the cathodes, a by-product stream composed of a sulfuric acid-based electrolyte containing dissolved copper and other impurities, mainly antimony and bismuth, is generated [11]. The sulfuric acid and copper present in the spent electrolysis baths are recovered and continuously reused in the electrorefining. To achieve this, the metallic impurities of Sb and Bi,

* Corresponding author.
E-mail address: mcmarti@iqn.upv.es (M.C. Martí-Calatayud).

https://doi.org/10.1016/j.jece.2024.112005
Received 26 October 2023; Received in revised form 12 January 2024; Accepted 19 January 2024
Available online 21 January 2024

which decrease the quality of the produced copper cathodes, are selectively removed by treating the electrolyte with aminophosphonic ion exchange resins [12,13]. Before reaching the column breakthrough capacity, the resins need to be regenerated using highly concentrated hydrochloric acid, which is capable to elute the impurities retained by ion exchange. As a result, an effluent that mainly contains antimony and bismuth is obtained [14,15], the treatment of which is of great interest both for the recovery of these critical metals and for the reuse of the acidic solution.

Usually, the effluent is treated by distillation to recover part of the HCl employed in the elution of the resins [16]. After that, the resulting liquor containing the metals is precipitated by addition of gypsum and deposited in landfills [17]. Another common treatment is to neutralize the eluate with lime; where the resulting product can be removed as toxic waste [14] or recovered as a metallic oxide that is sold as raw material to produce Sb-based flame retardants [18], or electrical-quality bismuth [19]. Currently, other processes to recover Sb and Bi from eluates of the ion exchange regeneration have been developed, such as liquid-liquid extraction [14] or selective precipitation by addition of NaOH and NH_4OH [20]. Most of the technologies mentioned require the addition of large quantities of chemicals, limit the continuous reuse of HCl as extractant and even entail the loss of Sb and Bi. In contrast with these techniques, electrodeposition can also be used for recovering metals from industrial and mining effluents [21,22], but implying a minimal addition of reagents. Recently, some authors have highlighted the feasibility of electrochemical deposition to achieve individual metal recovery from multicomponent electrolytes [23,24]. Thanu and Jayakumar [23] found an optimum potential and current at which Sb is electrodeposited individually from an electrolyte containing Sb, Bi and Fe. Grima et al. [24] implemented an electrodeposition process to recover the different metals contained in a multicomponent electrolyte composed of Ni, Co and Mn, separately. Individual recovery by electrodeposition can be feasible when, at a given potential, the reduction of one metal occurs, whereas the reduction of others does not occur [25,26]. That is, the selective recovery can be ensured by operating under potentiostatic control. For example, recovering nickel and copper separately is achievable because of the difference between their reduction potentials [27]. However, the selectivity of the process can also be modulated under galvanostatic control in the case that a selective separation is not feasible under potentiostatic mode.

In previous studies, the recovery of antimony from highly concentrated HCl solutions by means of electrodeposition has been investigated, by conducting a phenomenological characterization of the electrochemical reactions taking place under varying compositions and operating conditions [28], and by studying the role of mass transfer on the complete recovery of antimony by electrodeposition [29]. However, the presence of a competing dissolved metal in the composition of the effluents was not considered. In the present study, this important challenge is addressed, and the selective separation of antimony and bismuth from a highly concentrated HCl solution by electrodeposition is evaluated. The voltammetric response of solutions with varying concentrations of Sb and Bi is analyzed and the potentials at which different electrochemical reactions take place are identified. Subsequently, the selectivity and current efficiency of the metal recovery is evaluated in potentiostatic and galvanostatic mode using a reference composition that emulates that of the real effluents generated in the copper electrorefining. Moreover, two of the main factors that influence the selectivity of the galvanostatic process are investigated: the level of applied current density and the relative concentration of Sb versus Bi in the effluents.

2. Experimental

2.1. Materials and reagents

The reference solution used in the present study is composed of 10 mM Sb(III), 2.5 mM Bi(III) and 6 M HCl, which is based on the typical concentrations measured in the real effluent obtained as a result of the regeneration of aminophosphonic ion exchange resins at Chuquicamata mining sites (Chile) [4,30]. The use of highly concentrated HCl as eluent is justified by the low solubility of antimony and bismuth. Moreover, other concentrations of antimony and bismuth have also been used to analyze the effect of varying proportions between both elements in the electrochemical response of the system (mixtures of 5 mM Sb and 5 mM Bi, and mixtures of 2.5 mM Sb and 10 mM Bi) [14]. All solutions were prepared with analytical grade reagents, Sb_2O_3 (99%, Sigma Aldrich), Bi_2O_3 (99.9%, Sigma Aldrich) and HCl (37%, Panreac), and distilled water.

2.2. Experimental setup and voltammetric measurements

Cyclic voltammetry experiments were conducted using a three-electrode cell. A platinum plate enclosed in Teflon with an area of 0.071 cm^2 was used as the working electrode (Metrohm), the reference electrode was an Ag/AgCl (3 M KCl) electrode (Metrohm), and the counter electrode was a platinum ring with an area of 1 cm^2 (Mettler-Toledo).

Linear sweep voltammetry and electrolysis tests were conducted using an undivided reactor of 250 mL, also using a three-electrode configuration. In this case, a copper plate with 20 cm^2 of effective area was used as the cathode, an Ag/AgCl (3 M KCl) electrode was employed as reference electrode, and the anode was a dimensionally stable anode (DSA) composed of a sheet of titanium coated with a mixed metal oxide layer (RuO_2/IrO_2: 0.70/0.30), with an effective area of 40 cm^2. The experiments were carried out under hydrodynamic conditions using a magnetic stirrer with controlled stirring rate (500 rpm).

The cyclic and linear voltammetric measurements were obtained at a scan rate of 10 mV s^{-1}, beginning at the open circuit potential (OCP) towards cathodic potentials. For linear voltammetry, the cathodic limit potential was $-0.65\ V_{Ag/AgCl}$. For cyclic voltammetry, the potential range was $+0$ to $-0.6\ V_{Ag/AgCl}$; in this case, when the cathodic limit potential is reached, the scan is inverted until the anodic limit potential is reached. In cyclic voltammetry, several cycles are required to stabilize the system and obtain reproducible results.

The voltammetric study was carried out with three different solutions. First, the reference solution was analyzed, and then voltammetry was performed with a 6 M HCl solution with 10 mM Sb and another one with 2.5 mM Bi to obtain the electrochemical response of both elements separately (in the absence of the corresponding competing metal). All experiments were conducted at room temperature (25 °C) employing a potentiostat/galvanostat (Autolab PGSTAT 302 N) and NOVA 1.10 software.

2.3. Electrodeposition experiments

Electrolysis experiments were conducted with the reference solution in potentiostatic and galvanostatic mode. The applied values of potential and current density were selected according to the results obtained previously in the voltammetric experiments. In galvanostatic mode, the effect of applying different current density values on the selectivity was studied. After that, experiments were carried out varying the molar fraction of antimony, calculated as $x_{Sb} = \frac{c_{Sb}(0)}{c_{Sb}(0)+c_{Bi}(0)}$, to evaluate the influence of different proportions between Sb and Bi on the selectivity of the process. This effect was tested at high and low levels of current density. The duration of the experiments was 3 h.

The concentrations of bismuth and antimony of samples taken from the electrochemical reactor were measured by atomic absorption spectroscopy (Perkin-Elmer model AAnalyst 100). To obtain the concentration of antimony, an antimony hollow cathode lamp (Varian Techtron Pty. Ltd.) was used at a wavelength of 217.6 nm. For the determination of bismuth, a bismuth hollow cathode lamp was employed (Varian

Techtron Pty. Ltd.) at a wavelength of 223.1 nm. In both cases, a spectral bandwidth of 0.2 nm, a current of 15 mA and an acetylene-air ratio of 2:4 were used.

The morphology and composition of the deposits were analyzed by scanning electron microscopy (SEM, Zeiss model Ultra 55) and an energy dispersive X-ray analyzer attached to the SEM, respectively. The applied acceleration voltage was 10 kV.

The selectivity or separation efficiency of Sb over Bi (S_{Bi}^{Sb}) has been calculated according to Eq. 1, in which, the progress of each metal deposition in terms of relative concentrations is compared [31]:

$$S_{Bi}^{Sb}(t) = \frac{\left[\frac{c_{Bi}(t)}{c_{Bi}(0)}\right] - \left[\frac{c_{Sb}(t)}{c_{Sb}(0)}\right]}{\left[1 - \frac{c_{Bi}(t)}{c_{Bi}(0)}\right] + \left[1 - \frac{c_{Sb}(t)}{c_{Sb}(0)}\right]} \quad (1)$$

where c_{Bi} and c_{Sb} are the concentration of bismuth and antimony in the solution ($molL^{-1}$) at the beginning of the experiments (0) and at a specific time (t). The values of S_{Bi}^{Sb} vary between − 1, where only the electrodeposition of Bi occurs, and + 1 for the completely selective electrodeposition of Sb.

The evolution of current efficiency (Φ) of each metal (Φ_{Sb} and Φ_{Bi}) has been determined using Eq. 2 and Eq. 3, respectively, where n represents the number of electrons involved in the deposition ($n = 3$ for both metals); F is the Faraday constant (96,485.33 C mol^{-1}); V is the reactor volume (L); and $I(t)$ represents the function of the current with time (A). The total electrodeposition current efficiency ($\Phi_{electrodeposition}$) has been calculated as the sum of both current efficiencies (Eq. 4).

$$\Phi_{Sb}(t) = \frac{n \quad F \quad V(c_{Sb}(0) - c_{Sb}(t))}{\int_0^t I(t)dt} \quad 100(\%) \quad (2)$$

$$\Phi_{Bi}(t) = \frac{n \quad F \quad V(c_{Bi}(0) - c_{Bi}(t))}{\int_0^t I(t)dt} \quad 100(\%) \quad (3)$$

$$\Phi_{electrodeposition}(t) = \Phi_{Sb}(t) + \Phi_{Bi}(t) \quad (4)$$

3. Results and discussion

3.1. Voltammetric study

Fig. 1 shows the three cyclic voltammograms of 6 M HCl solutions with different concentrations of Sb and Bi: the reference solution containing both metals and two additional solutions, one containing only antimony (10 mM) and another one with only bismuth (2.5 mM).

Starting the analysis of the voltammograms with the cathodic scan, from the OCP towards negative potentials, for the solution containing only Sb, a reduction peak can be seen at − 0.32 $V_{Ag/AgCl}$, while the reduction peak for solutions containing only Bi appears at less cathodic potentials, around − 0.27 $V_{Ag/AgCl}$. The predominant species of Sb and Bi in 6 M HCl solutions are the chloro complexes $SbCl_6^{3-}$ and $BiCl_5^{2-}$ (see **Fig. S. 1.** in Supplementary material), so their electrodeposition occurs mainly according to Eq. 5 and Eq. 6, respectively [29].

$$SbCl_6^{3-} + 3e^- \longrightarrow Sb + 6Cl^- \quad (5)$$

$$BiCl_5^{2-} + 3e^- \longrightarrow Bi + 5Cl^- \quad (6)$$

Regarding the voltammogram obtained with the mixture solution (Sb + Bi), only one reduction peak is also observed. This may indicate that the electrodeposition of both elements takes place simultaneously producing an alloy in the surface of the electrode, as indicated by Eq. 7 [32].

$$x \quad BiCl_5^{2-} + y \quad SbCl_6^{3-} + 3\cdot(x+y) \quad e^- \longrightarrow Bi_xSb_y + (5x+6y) \quad Cl^- \quad (7)$$

The potential of the reduction peak of the mixture (−0.29 $V_{Ag/AgCl}$) lies in between the values obtained for the solutions containing only one metal. A zoom of the reduction peaks is shown in the inset of Fig. 1, where it can be clearly seen that the reduction of Bi appears at less cathodic potentials as compared to Sb, while that of the mixture takes place at intermediate potentials. Another remarkable fact is the high current density of the reduction peak of Bi (6.8 mA cm^{-2}) as compared to the other two systems (4.8 and 4.7 mA cm^{-2}), in spite of the lower concentration of Bi. The reason for that can be the higher diffusion coefficient of bismuth versus antimony. Schoenleber et al. [33] obtained values for the Bi diffusion coefficient in different media that almost double those obtained for Sb. In all cases, after the reduction peak, the current signal decays reaching highly negative values in the potential range between − 0.50 and − 0.60 $V_{Ag/AgCl}$, which denotes the vigorous generation of hydrogen bubbles due to the hydrogen evolution reaction (HER), as a consequence of the reduction of the electrolyte solution [28].

In the anodic scan, once the potential has been reversed, a main oxidation peak can be observed for the three systems. The oxidation peaks correspond to the reverse reactions of Eq. 5, Eq. 6 and Eq. 7, that is, to the redissolution of the electrodeposited metals previously formed during the cathodic scan.

To analyze the reduction process of the elements separately and in the mixture in more detail, linear sweep voltammetry tests were executed (Fig. 2). The experiments were carried out in the reactor employed for the electrodeposition tests, with the copper cathode and under hydrodynamic conditions. A previous study demonstrated the positive influence of working at convective regimes for the Sb electrodeposition [28]. The shape of the voltammograms is similar in all three systems; a sharp decrease in current density is observed at − 0.25 $V_{Ag/AgCl}$ for the solution with only Sb and the mixture, and at − 0.28 $V_{Ag/AgCl}$ for the solution only containing Bi as dissolved metal. In these voltammograms, a plateau is registered instead of a peak, because the dissolved metals are continuously supplied from the bulk solution to the electrode surface by convection. When the electrodeposition rate approaches the mass transport rate of dissolved metals towards the electrode, mass transfer becomes the limiting step of the process and a plateau at the corresponding limiting current density (i_L) is registered. Here, it is to note that, for the low level of metal concentrations of this study, similar i_L values around 3.0 mA cm^{-2} are obtained for the three solutions. Regarding the relevance of HER, this reaction starts to be

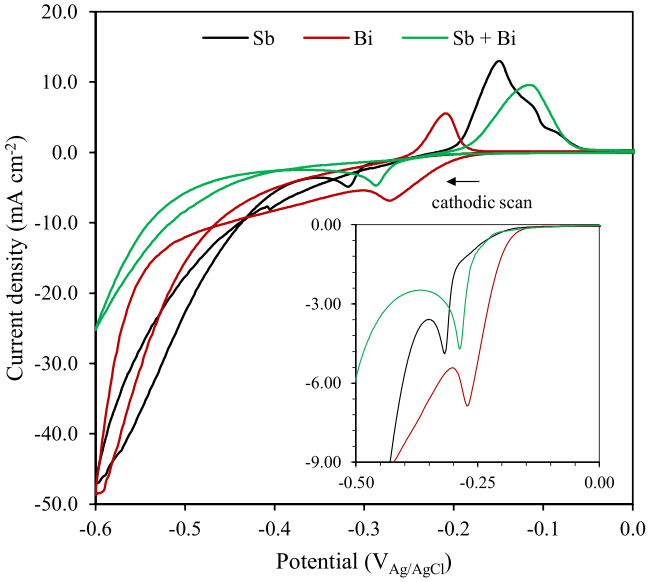

Fig. 1. Cyclic voltammogram of solutions with different concentrations of antimony and bismuth in 6 M HCl: 10 mM Sb (black line), 2.5 mM Bi (red line), and 10 mM Sb and 2.5 mM Bi mixtures (green line). Inset: Zoom of reduction peaks.

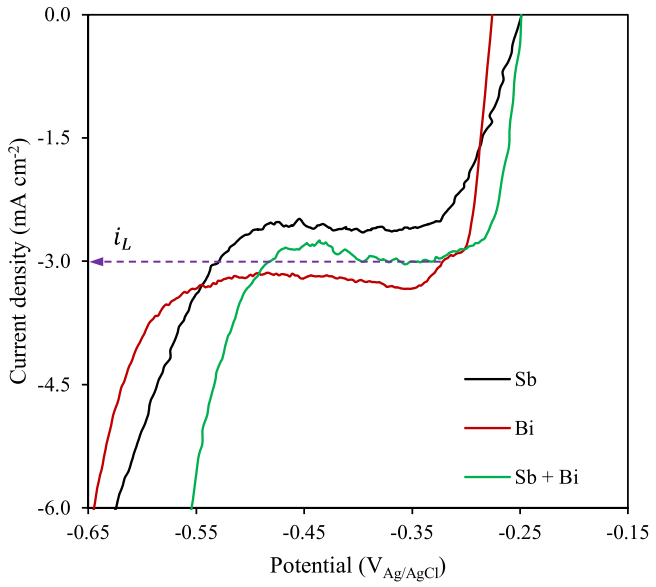

Fig. 2. Linear sweep voltammograms of solutions with different concentrations of antimony and bismuth in 6 M HCl: 10 mM Sb (black line), 2.5 mM Bi (red line), and mixtures of 10 mM Sb and 2.5 mM Bi (green line).

predominant at less cathodic potentials for the reference solution. Some authors have stated that Bi displaces the HER to more cathodic potentials [34].

3.2. Potentiostatic electrodeposition with the reference effluent composition

As observed in Fig. 2, the reduction potentials of antimony and bismuth are separated around 30 mV, beginning the bismuth reduction at more cathodic potentials than the antimony reduction. Thus, to check whether the separation of the elements by electroreduction experiments is feasible, a potentiostatic test was carried out at − 0.25 $V_{Ag/AgCl}$.

The results of this experiment can be observed in Fig. 3a, where the evolution of the relative concentration of each metal is represented. For both metals, the relative concentration diminishes with time. However, the relative amount of Bi electrodeposited is significantly lower than that of Sb. The selectivity of the process, calculated according to Eq. 1 based on the fittings of $c(t)/c(0)$ of Fig. 3a, is shown as a function of the electrodeposition time in Fig. 3b. It reveals an electrodeposition preference for antimony, in agreement with our initial expectations according to the linear voltammograms. Moreover, the high value of the $c_{Sb}(0)/c_{Bi}(0)$ ratio implies a higher availability of Sb(III) species near the electrode, what favors the preferential electrodeposition of this metal. Nevertheless, the selectivity does not reach a very high value (around 0.6); so, it can be concluded that it is not possible to separate antimony and bismuth in hydrochloric acid by operating in potentiostatic mode. These results are in line with the conclusions achieved in a previous study on Bi deposition by Martín-González et al. [35], who observed that underpotential codeposition of two metals occurs when the difference between the potentials for the two separate cations is lower than ~250 mV. In the mixtures investigated in the present work, the reduction potentials of antimony and bismuth are separated only by around 30 mV; what could be a limitation for the potentiostatic electrodeposition of the individual elements. At potentials less cathodic than − 0.25 $V_{Ag/AgCl}$ no metal would be deposited because the reduction of none of them takes place.

3.3. Galvanostatic electrodeposition with the reference effluent composition

After confirming that the separation of Sb and Bi by electrodeposition based on the different reduction potentials of each metal was not feasible operating in potentiostatic mode, a different approach was investigated. Instead of applying a potentiostatic control on the deposition process, a kinetic control was searched by operating in galvanostatic mode. Galvanostatic tests at current densities, below, approximately equal to, and above the i_L value obtained from Fig. 2 (3 mA cm^{-2}) were performed. The evolution of the relative concentrations of both dissolved metals in the reactor for the three applied current densities is shown in Fig. 4. As can be seen in Fig. 4a, the decrease of Sb concentration in the reactor becomes progressively faster with an increase in the applied current density, this indicating that the rate of Sb electrodeposition increases at high current densities. This effect is contrary to that observed in a previous work, where an electrodeposition deceleration of Sb was detected at increasing current densities in an HCl solution containing Sb [29]; this trend changes with the presence of Bi. The same effect is observed in the case of Bi (Fig. 4b). However, at the current density below i_L, 1.5 mA cm^{-2}, the concentration of dissolved Bi remains practically constant with time, meaning that only Sb could be electrodeposited under these conditions. During this test, the measured electrode potential is approximately − 0.24 $V_{Ag/AgCl}$ (see Fig. S. 2 in Supplementary material). So, the results agree with those obtained in potentiostatic mode at − 0.25 $V_{Ag/AgCl}$. The registered electrode potential (less cathodic than the reduction potential of bismuth) and the ratio between the concentrations of both metals seem to be the main factors affecting the selectivity of the process. However, an increase in the

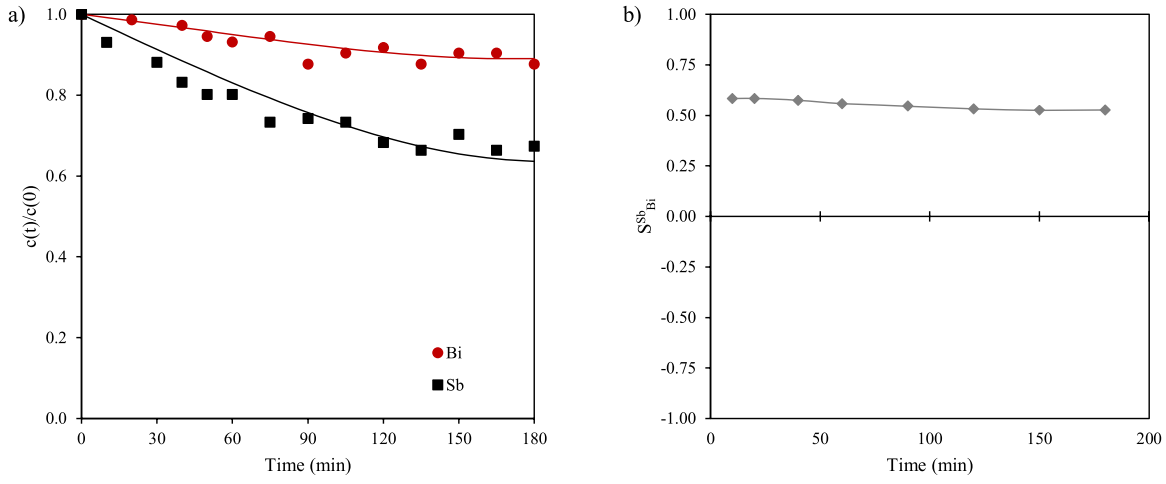

Fig. 3. Evolution of the relative concentration of antimony and bismuth (a); and, of the selectivity of antimony over bismuth (b) at − 0.25 $V_{Ag/AgCl}$.

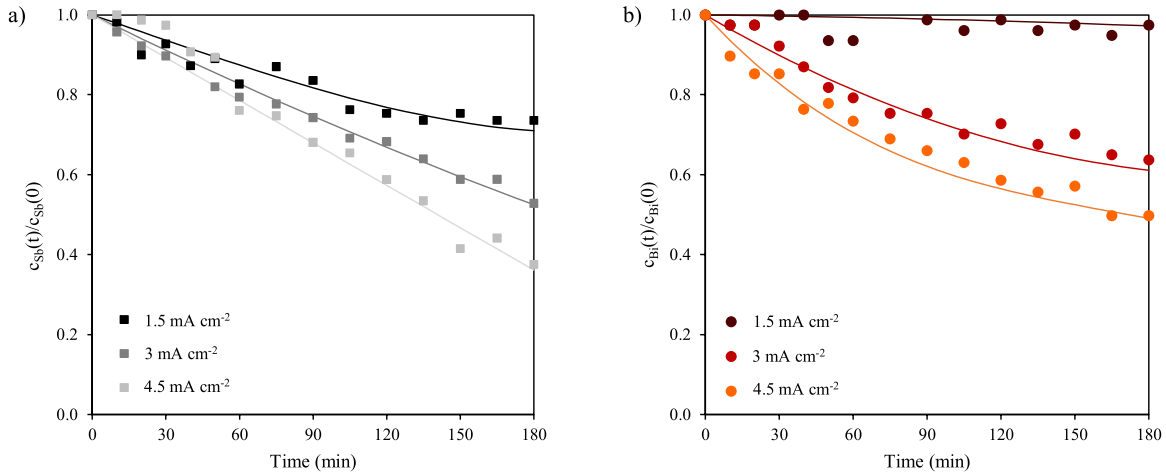

Fig. 4. Evolution of the relative concentration of antimony (a) and bismuth (b) at different applied current densities with the reference solution: mixtures of 10 mM Sb and 2.5 mM Bi in 6 M HCl.

applied current density notably accelerates the Bi electrodeposition, which coincides with the registration of electrode potentials higher than the reduction potential of Bi, $-0.27\ V_{Ag/AgCl}$ at 3 mA cm^{-2} and $-0.30\ V_{Ag/AgCl}$ at 4.5 mA cm^{-2} (Fig. S. 2 of Supplementary material), and similar $c(t)/c(0)$ values for both metals are obtained. Thus, it seems that the limited supply of dissolved Sb towards the electrode by operating at $i > i_L$ together with the more cathodic potentials reached at high currents, promote an acceleration of the electrodeposition of Bi and decrease the process selectivity towards Sb.

The selectivity of the process (shown in Fig. 5) was calculated according to Eq. 1 using the fittings of the relative concentration of each metal. As mentioned above, at $i_{applied} < i_L$ a highly selective antimony deposition is confirmed with S_{Bi}^{Sb} values larger than 0.9. By operating under conditions where mass transfer is not a limiting process, the supply of dissolved antimony towards the electrode is fast enough to satisfy the imposed current density, and the electrons released at the electrode surface can be accepted by Sb(III) species. This results in a selective process for the reduction of antimony, which is the less cathodic reaction according to the voltammograms of Fig. 2 and agrees well with the electrode potentials close to $-0.24\ V_{Ag/AgCl}$ registered for

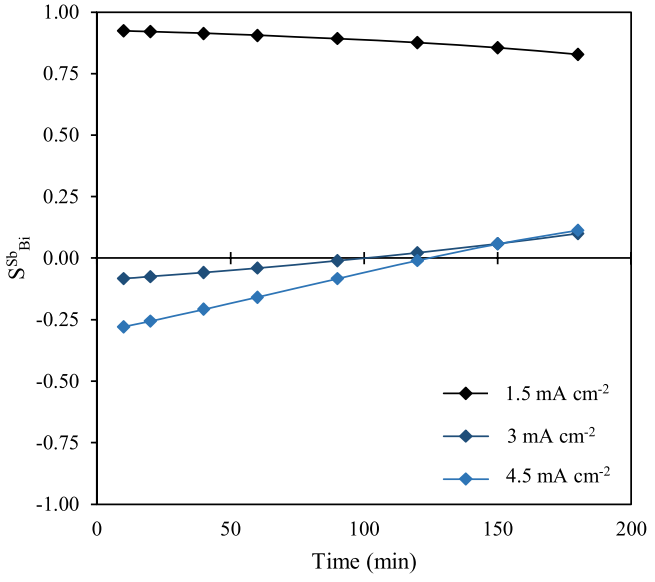

Fig. 5. Selectivity of antimony over bismuth at different applied current densities.

this experiment. At such potential values the reduction of bismuth is almost absent, thus resulting in a very selective process. However, an important change in the process selectivity occurs for the range $i_{applied} \geq i_L$. In these cases, the process is not selective for either metal (S_{Bi}^{Sb} values are close to 0), where two counteracting phenomena seem to play a role on the metal recovery. Whereas the high $c_{Sb}(0)/c_{Bi}(0)$ ratio may favor the deposition of Sb; by operating at high current densities, the deposition of antimony is more limited by mass transfer, while Bi electrodeposition becomes faster. This is in agreement with the larger current densities obtained in the voltammograms for the solution only containing Bi (Fig. 2).

The current efficiencies of the process for antimony and bismuth are presented in Fig. 6a and b, respectively. The values obtained for bismuth are below those for antimony as a consequence of the lower concentrations of Bi in the solution ($c_{Sb}(0)/c_{Bi}(0) = 4$), and the total amount of Bi removed is more than four times lower than that of Sb (see Fig. S. 3 in Supplementary material). For both elements, the current efficiency decreases with time and applied current density because of the higher contribution of the HER. Note that the current efficiency of Bi at 1.5 mA·cm^{-2} has not been estimated because the deposition of this metal is insignificant at this current density. Regarding the total current efficiencies (see Fig. S. 4 in Supplementary material), which are calculated as the sum of $\Phi_{Sb} + \Phi_{Bi}$, the average values obtained at $i_{applied} \leq i_L$ are similar (75.6% at 1.5 mA cm^{-2} and 70.5% at 3 mA cm^{-2}); however, this value drops at 4.5 mA cm^{-2} (48.6%). Thus, it can be concluded that, when the limiting current density is exceeded, HER is favored decreasing the overall electrodeposition efficiency. Moreover, the increased predominance of HER with the reaction time can be a consequence of the gradual depletion of dissolved metals near the electrode surface.

Although the main aim of this study is to investigate the selectivity of the process, it is remarkable that the complete recovery of antimony and bismuth would require longer operating times, for which high values of total current efficiency could not be sustained under the applied current densities. In our previous study dealing with the deposition of antimony in highly concentrated HCl solutions, it was demonstrated that mass transfer is a limiting phenomenon for this process [29]. The actual limiting current density for an electrodeposition process changes with time with the decrease in the concentration of dissolved metal according to Eq. 8:

$$i_L(t) = n \cdot F \cdot k_m \cdot c(t) \tag{8}$$

Where $i_L(t)$ refers to the actual value of the limiting current density, and k_m to the mass transfer coefficient. Consequently, as the gradual decrease in concentration of the dissolved metal occurs, the actual value

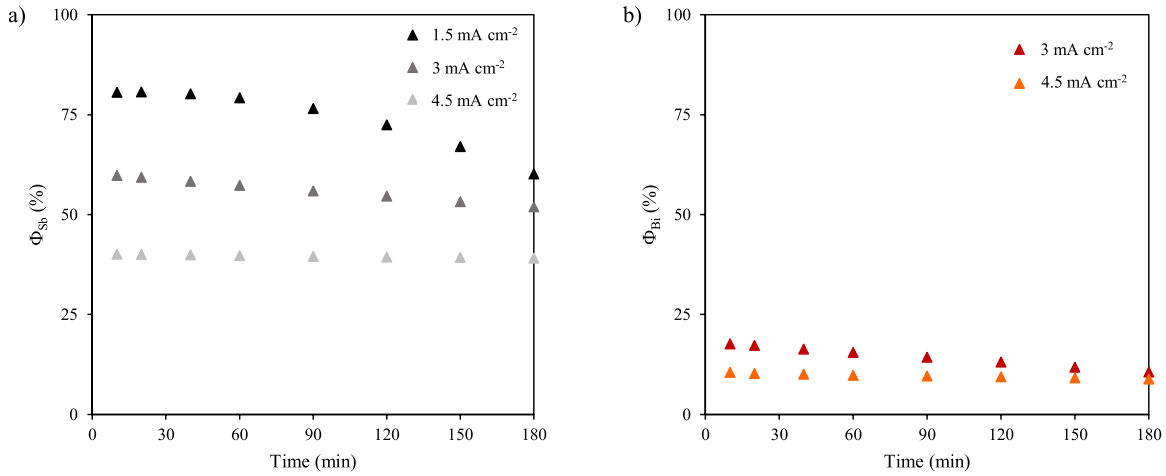

Fig. 6. Evolution of the current efficiency at different applied current densities for antimony (a) and for bismuth (b).

of limiting current density may fall below the applied one, this causing an intensification of other electrochemical reactions, such as HER. Nonetheless, in our previous study, the complete recovery of antimony could be achieved ensuring a high current efficiency by operating at lower values of current density [29]. In consequence, a possible operating strategy would be to conduct the electrodeposition process in two phases at different applied current densities: a first phase where an electrode rich in antimony is obtained, and a second one at lower current densities where the complete recovery of the metals is achieved ensuring high current efficiencies and enabling the recycling of the acidic solution.

3.4. Galvanostatic electrodeposition with different concentration ratios between Sb and Bi

The concentration of metals in the effluent resulting from the regeneration of the aminophosphonic ion exchange resins with hydrochloric acid can vary depending on the origin of the copper ores and the procedure followed during the regeneration stage [4,14]. Therefore, it is interesting to investigate whether the conclusions obtained for the reference solution composition would apply for other proportions of Sb and Bi. The selectivity of the process has been further investigated at different proportions of Sb and Bi: one with the same concentration of both metals, and another one with a higher concentration of Bi with respect to Sb. The three $c_{Sb}(0)/c_{Bi}(0)$ ratios and corresponding molar fractions of Sb are summarized in Table 1.

Fig. 7 shows the voltammograms obtained with solutions with different $c_{Sb}(0)/c_{Bi}(0)$ ratios. When analyzing the voltammograms from OCP towards cathodic potentials, a reduction peak is observed. The peak potential shifts slightly towards more cathodic values as the $c_{Sb}(0)/c_{Bi}(0)$ ratio decreases, and its current density increases notably for $c_{Sb}(0)/c_{Bi}(0) = 0.25$ (when Bi is the predominating dissolved metal). When the scan is inverted, the oxidation peak is detected in all cases, and a change in peak area with the Bi concentration occurs, similar as that observed for the reduction peak. The results agree with those shown in Fig. 1: a higher proportion of Bi implies an increase in peak current density.

The electrodeposition tests have been executed at two current densities chosen based on the selectivity measured in the previous section:

Table 1
Composition of the investigated solutions.

Sb (III) (mM)	Bi (III) (mM)	HCl (M)	$c_{Sb}(0)/c_{Bi}(0)$	x_{Sb}
10	2.5	6	4	0.8
5	5	6	1	0.5
2.5	10	6	0.25	0.2

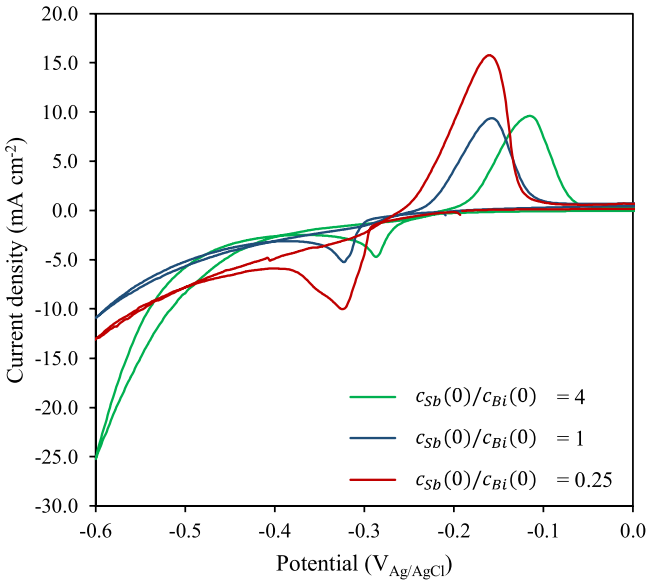

Fig. 7. Cyclic voltammogram of solutions with various concentration ratios between Sb and Bi in 6 M HCl.

1.5 mA·cm^{-2}, which are conditions that favor the selectivity towards antimony; and 4.5 mA·cm^{-2}, where the process is not selective.

When the applied current density is 1.5 mA cm^{-2}, see Fig. 8a, the electrodeposition of Sb is similar for all three ratios analyzed, the amount of Sb removed is higher with a larger proportion of Sb in the initial solution (Fig. S. 7 a in Supplementary material). The rate of Bi deposition increases slightly when the x_{Sb} diminishes (Fig. 8b), even though Sb electrodeposition predominates at this low value of current density (Fig. S. 7 a). For $x_{Sb} \leq 0.5$, the electrode potential reaches the Bi reduction potential (Fig. S. 5), what explains the increased removal of Bi as the proportion of this metal in the solution increases. Focusing on the total amount removed of each metal at 1.5 mA cm^{-2} for $x_{Sb} = 0.8$, the amount of Sb removed is notably higher than Bi. Therefore, these conditions could be applied to recover Sb selectively, as was also noted by the selectivity values of Sb over Bi, greater than 0.9 (Fig. 10 a).

The evolution of the relative concentration of Sb and Bi at 4.5 mA cm^{-2} is shown in Fig. 9a and b, respectively. For both metals, the relative concentration diminishes with time in a similar trend for the three x_{Sb} values, confirming that at high current densities, the process is not selective for either metal, regardless of their relative concentration in solution. Furthermore, the electrode potential reached for all x_{Sb}

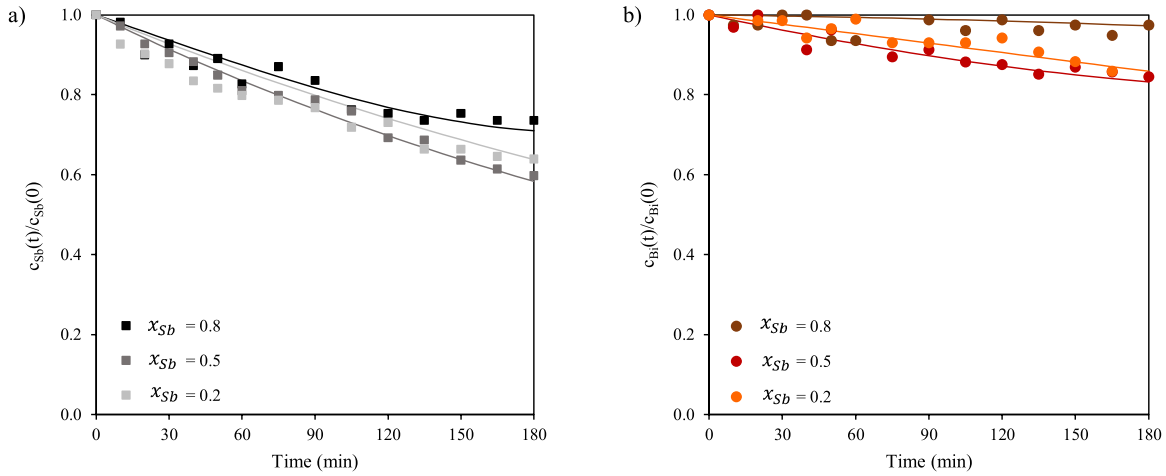

Fig. 8. Evolution of the relative concentration of antimony (a) and bismuth (b) at 1.5 mA cm^{-2} in solutions with different molar fractions of antimony.

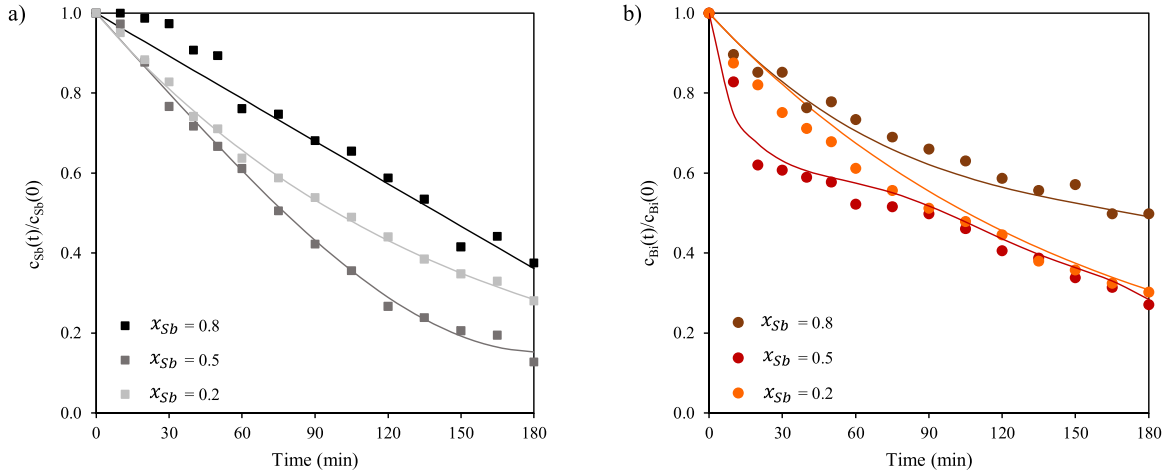

Fig. 9. Evolution of the relative concentration of antimony (a) and bismuth (b) at 4.5 mA cm^{-2} in solutions with different molar fractions of antimony.

values is also very similar, and close to the Bi reduction potential (Fig. S. 6 in Supplementary material).

The selectivity of the process has been obtained for both applied current densities. The selectivity at 1.5 mA cm^{-2} is shown in Fig. 10 a, where the results obtained confirm that at low current densities, the Sb deposition predominates over the Bi deposition. However, this predominance decreases when the x_{Sb} diminishes. On the contrary, the results obtained at 4.5 mA cm^{-2} (Fig. 10 b) support the conclusion that at high current densities there is no prevalence in the deposition of any metal, with independence of their relative concentration. Under such

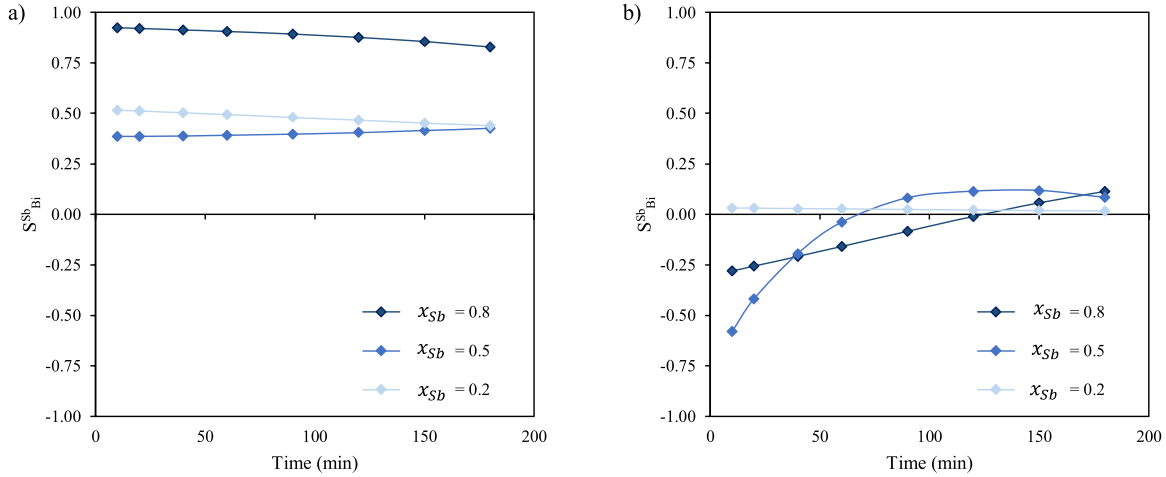

Fig. 10. Selectivity of antimony over bismuth at 1.5 mA cm^{-2} (a) and 4.5 mA cm^{-2} (b) in solutions with different molar fractions of antimony.

conditions, the system evolves towards more cathodic electrode potentials, making feasible the electrodeposition of bismuth and causing a drop in selectivity. The electrons released at the cathode react with the electroactive species that are present near its surface, in nearly the same proportion as their concentration in the solution.

The analysis of the composition of the deposits (Fig. S. 9 and Table S. 1) confirms the above statements. The Sb deposition prevails over Bi when the applied current density is 1.5 mA cm^{-2}: for a molar proportion of 4 in the initial solution, a very high ratio of antimony vs. bismuth of 14.52 is reached in the final deposit. The process is still selective for the deposition of antimony for $c_{Sb}(0)/c_{Bi}(0) = 0.25$ and 1.5 mA cm^{-2}, with a final proportion reached in the deposit of 0.33, although a substantial drop in selectivity takes place. On the contrary, at 4.5 mA cm^{-2} the proportion of the metals in the initial solution and in the deposits is practically the same, so that it is confirmed that there is no preference for any element. Thanu and Jayakumar [23] obtained a similar conclusion working at high current densities (around 20 mA cm^{-2}) with a solution containing similar concentrations of Sb and Bi: they did not detect electrodeposition preference towards any metal. According to the presented results, it can be concluded that x_{Sb} is a relevant parameter when the galvanostatic electrodeposition is carried out at low current densities, verifying the importance of mass transfer in the electrodeposition process [29]. Other authors have highlighted the relevance of the relative concentrations of Sb and Bi in solution on the composition of the obtained deposits [36].

The current efficiencies for the electrodeposition of each metal have been calculated for both current densities (Fig. 11). In general, from all panels of Fig. 11, it can be concluded that a higher concentration of the element in the solution implies higher values of current efficiency for its specific deposition. In the case of Sb (Fig. 11 a, b), the highest current efficiency is obtained with the solutions with a predominance of Sb; and the analogous trend occurs for Bi (Fig. 11 c, d). This trend clearly agrees with that obtained for the total amount of removed metals represented as a function of the fraction of dissolved metals in the solutions (x_{Sb}), which are shown in Fig. S. 7 of the Supplementary material.

Focusing on the current efficiencies reached for Sb (Fig. 11 a, b), they decrease with the applied current density. This occurs because both reactions competing with the Sb deposition, the HER and the Bi deposition, are more relevant under conditions where the electrode potential reaches more cathodic values (Fig. S. 6 in Supplementary material). These effects are also confirmed when Φ_{Bi} is analyzed at different current densities (Fig. 11 c, d); for all x_{Sb}, it is observed that when current density increases, the current efficiency for Bi deposition also increases because the reduction potential of Bi is reached.

The evolution of the total current efficiency with different x_{Sb} values at both current densities (Fig. S. 8) confirms the previous statement. For high proportions of Bi, the overall deposition efficiency increases with current density, because the Bi electrodeposition is favored, and this metal is available in the solution at high concentrations. As mentioned above, this is consistent with the larger diffusion coefficients reported by Schloenleber et al. for bismuth species [33]. Therefore, higher current densities can be better sustained by bismuth, as the rate of supply of this metal towards the electrode may be higher than the rate of supply of antimony. This difference in transport rates of both metals would

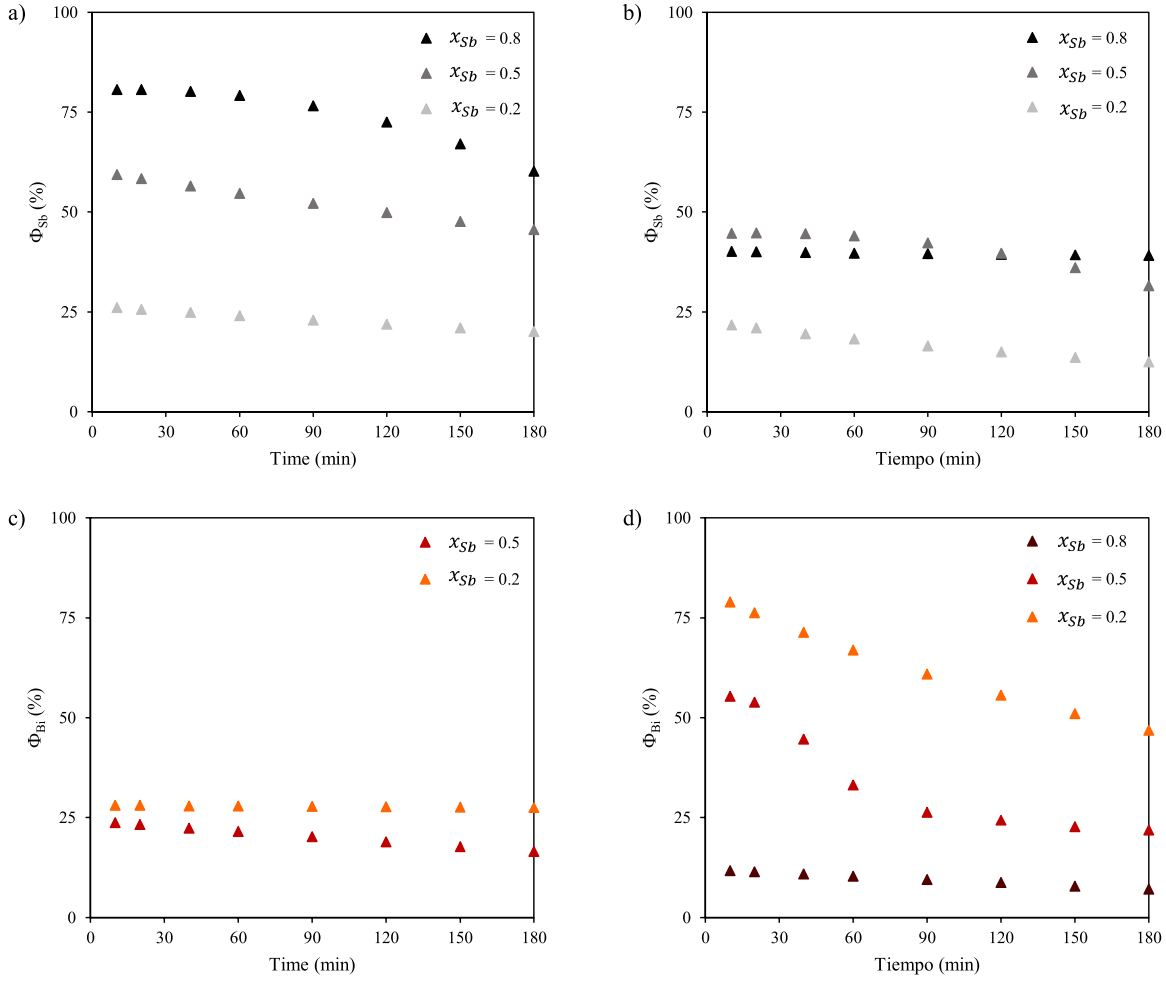

Fig. 11. Evolution of the current efficiency at different applied current for antimony at 1.5 mA cm^{-2} (a) and 4.5 mA cm^{-2} (b); and, for bismuth at 1.5 mA cm^{-2} (c) and 4.5 mA cm^{-2} (d), in solutions with different molar fractions of antimony.

explain the lower relevance of HER in systems where the concentration of Bi is higher than that of Sb. However, for the highest proportion of Sb in solution (x_{Sb} = 0.8), although the Bi electrodeposition may be favored, the low concentrations of Bi in solution, imply that the main reaction favored at high current densities is the HER. For this proportion, the overall deposition current efficiency drops from an average value of 75.6% at 1.5 mA cm^{-2} to a value of 49.2% at 4.5 mA cm^{-2}.

4. Conclusions

In this study, the selectivity of the electrodeposition of antimony and bismuth from highly concentrated hydrochloric acid solutions is analyzed. These solutions emulate the composition of eluates of ion exchange resins used to purify spent electrorefining baths. It has been found from a preliminar voltammetric analysis that the slight difference between the reduction potentials of antimony and bismuth makes the individual recovery of both metals a very challenging task. This conclusion was confirmed in potentiostatic electrolysis experiments at low cathodic potentials (i.e., −0.25 $V_{Ag/AgCl}$), which lie below the reduction potential of bismuth. On the contrary, very high selectivity factors of antimony vs. bismuth were achieved by operating in galvanostatic mode at current densities below the i_L for the reference solution composition. The electrode potentials reached under these conditions (unfavorable for the bismuth reduction) and the higher availability of antimony in the reference solution almost impede the deposition of bismuth. These promising results prove the feasibility of a highly selective recovery process by electrodeposition, which would improve the circularity of copper electrorefining. At current densities above i_L, a sharp drop in selectivity and also in the current efficiency for the antimony electrodeposition takes place, which is attributed to the higher cathodic potentials reached, that favor the deposition of bismuth and also the evolution of hydrogen. Galvanostatic experiments carried out at different proportions of antimony and bismuth showed that a higher proportion of bismuth increases the current efficiency for the deposition of this metal, thus decreasing the process selectivity. Operating at high current densities (4.5 mA cm^{-2}) involve reaching high cathodic potentials, and under these conditions, when the proportion of bismuth is low, the main reaction favored is the HER. On the contrary, when the availability of bismuth is high, overall electrodeposition efficiencies higher than 75% were reached working at high currents, although an unselective metal codeposition took place.

Declaration of Competing Interest

The authors declare that they have no known competing financial interests or personal relationships that could have appeared to influence the work reported in this paper.

Data availability

Data will be made available on request.

Acknowledgments

The authors thank the financial support from the Agencia Estatal de Investigación (AEI/10.13039/501100011033) (Spain) under the project PCI2019–103535 and by FEDER A way of making Europe. Funding for open access charge: CRUE-Universitat Politècnica de València.

Appendix A. Supporting information

Supplementary data associated with this article can be found in the online version at doi:10.1016/j.jece.2024.112005.

References

[1] G.A. Flores, C. Risopatron, J. Pease, Processing of complex materials in the copper industry: challenges and opportunities ahead, JOM 72 (2020) 3447–3461, https://doi.org/10.1007/s11837-020-04255-9.
[2] L. Li, D. Pan, B. Li, Y. Wu, H. Wang, Y. Gu, T. Zuo, Patterns and challenges in the copper industry in China, Resour. Conserv Recycl 127 (2017) 1–7, https://doi.org/10.1016/j.resconrec.2017.07.046.
[3] D. Dupont, S. Arnout, P.T. Jones, K. Binnemans, Antimony recovery from end-of-life products and industrial process residues: a critical review, J. Sustain. Metall. 2 (2016) 79–103, https://doi.org/10.1007/s40831-016-0043-y.
[4] K.S. Barros, V.S. Vielmo, B.G. Moreno, G. Riveros, G. Cifuentes, A.M. Bernardes, Chemical composition data of the main stages of copper production from sulfide minerals in Chile: a review to assist circular economy studies, Minerals 12 (2022), https://doi.org/10.3390/min12020250.
[5] T.E. Graedel, R. Barr, C. Chandler, T. Chase, J. Choi, L. Christoffersen, E. Friedlander, C. Henly, C. Jun, N.T. Nassar, D. Schechner, S. Warren, M.Y. Yang, C. Zhu, Methodology of metal criticality determination, Environ. Sci. Technol. 46 (2012) 1063–1070, https://doi.org/10.1021/es203534z.
[6] European Commission, European Commission, Report on critical raw materials and the circular economy, 2018, 2018. ⟨https://doi.org/10.2873/331561⟩.
[7] U.S. Geological Survey, 2022 Final list of critical minerals, Fed Regist 87 (2022) 10381–10382.
[8] N. Bolan, M. Kumar, E. Singh, A. Kumar, L. Singh, S. Kumar, S. Keerthanan, S. A. Hoang, A. El-Naggar, M. Vithanage, B. Sarkar, H. Wijesekara, S. Diyabalanage, P. Sooriyakumar, A. Vinu, H. Wang, M.B. Kirkham, S.M. Shaheen, J. Rinklebe, K.H. M. Siddique, Antimony contamination and its risk management in complex environmental settings: a review, Environ. Int. 158 (2022), https://doi.org/10.1016/j.envint.2021.106908.
[9] S. Dembele, A. Akcil, S. Panda, Technological trends, emerging applications and metallurgical strategies in antimony recovery from stibnite, Min. Eng. 175 (2022) 107304, https://doi.org/10.1016/J.MINENG.2021.107304.
[10] T. Dai, Y. Zhao, X.H. Ning, R. Lakshmi Narayan, J. Li, Z. wei Shan, Capacity extended bismuth-antimony cathode for high-performance liquid metal battery, J. Power Sources 381 (2018) 38–45, https://doi.org/10.1016/j.jpowsour.2018.01.048.
[11] A. Artzer, M. Moats, J. Bender, Removal of antimony and bismuth from copper electrorefining electrolyte: part II — an investigation of two proprietary solvent extraction extractants, JOM 2018 70 (12) (2018) 2856–2863, https://doi.org/10.1007/S11837-018-3129-0.
[12] D. Luo, M. Fernández de Labastida, J.L. Cortina, J. Lopez, Recovery of antimony and bismuth from arsenic-containing waste streams from the copper electrorefining circuit: an example of promoting critical metals circularity from secondary resources, J. Clean. Prod. 415 (2023) 137902, https://doi.org/10.1016/j.jclepro.2023.137902.
[13] E. Díaz, J.A. Maldonado Calvo, J.M. Gallardo, A. Paúl, Extraction of antimony from a hydrochloric acid side stream of copper electro-refining by hydrolysis, Hydrometallurgy 219 (2023), https://doi.org/10.1016/j.hydromet.2023.106076.
[14] N. Benabdallah, D. Luo, M. Hadj Youcef, J. Lopez, M. Fernández de Labastida, A. M. Sastre, C.A. Valderrama, J.L. Cortina, Increasing the circularity of the copper metallurgical industry: recovery of Sb(III) and Bi(III) from hydrochloric solutions by integration of solvating organophosphorous extractants and selective precipitation, Chem. Eng. J. 453 (2023) 10–14, https://doi.org/10.1016/j.cej.2022.139811.
[15] K. Santana, A. Luiz, V. Machado, V. Schaeffer, S. Velizarov, Membrane electrolysis for recovering Sb and Bi from elution solutions of ion-exchange resins used in copper electrorefining: a cyclic voltammetric study, J. Electroanal. Chem. 924 (2022) 116867, https://doi.org/10.1016/j.jelechem.2022.116867.
[16] T. Nagai, Purification of copper electrolyte by solvent extraction and ion-exchange techniques, Miner. Process. Extr. Metall. Rev. 17 (1997) 143–168, https://doi.org/10.1080/08827509708914145.
[17] G. Cifuentes, M. Agurto, S. Di, I. Gentico, M. Cifuentes-Cabezas, Antimony recovery by electro-electrodialysis (EED), 2019. ⟨https://doi.org/10.19080/IJESNR.2022.31.556310⟩.
[18] A. Artzer, M. Moats, J. Bender, Removal of antimony and bismuth from copper electrorefining electrolyte: part I — a review, JOM 70 (2018) 2033–2040, https://doi.org/10.1007/s11837-018-3075-x.
[19] K.C. Sole, M.B. Mooiman, E. Hardwick, Ion exchange in hydrometallurgical processing: an overview and selected applications, Sep. Purif. Rev. 47 (2018) 159–178, https://doi.org/10.1080/15422119.2017.1354304.
[20] E. Díaz Gutiérrez, J.A. Maldonado Calvo, J.M. Gallardo Fuentes, A. Paúl Escolano, Effect of pH hydrolysis on the recovery of antimony from spent electrolytes from copper production, Materials 16 (2023) 1–12, https://doi.org/10.3390/ma16113918.
[21] J. Carrillo-Abad, M. Garcia-Gabaldon, I. Ortiz-Gandara, E. Bringas, A.M. Urtiaga, I. Ortiz, V. Perez-Herranz, Selective recovery of zinc from spent pickling baths by the combination of membrane-based solvent extraction and electrowinning technologies, Sep Purif. Technol. 151 (2015) 232–242, https://doi.org/10.1016/j.seppur.2015.07.051.
[22] G. Stando, P.M. Hannula, B. Kumanek, M. Lundström, D. Janas, Copper recovery from industrial wastewater - synergistic electrodeposition onto nanocarbon materials, Water Resour. Ind. 26 (2021), https://doi.org/10.1016/j.wri.2021.100156.
[23] V.R.C. Thanu, M. Jayakumar, Electrochemical recovery of antimony and bismuth from spent electrolytes, Sep Purif. Technol. 235 (2020) 116169, https://doi.org/10.1016/j.seppur.2019.116169.

[24] L. Grima-Carmena, S. Oyonarte-Andrés, J.J. Giner-Sanz, M. García-Gabaldón, F. Bosch-Mossi, V. Pérez-Herranz, Statistical analysis of the effect of the electrochemical treatment and the acid concentration on the leaching of NMC cathodes from spent Li-ion batteries, J. Environ. Chem. Eng. 11 (2023) 110423, https://doi.org/10.1016/j.jece.2023.110423.
[25] R.D. Armstrong, M. Todd, J.W. Atkinson, K. Scott, Selective electrodeposition of metals from simulated waste solutions, J. Appl. Electrochem. 26 (1996) 379–384.
[26] M. García-Gabaldón, V. Pérez-Herranz, J. García-Antón, J.L. Guiñón, Electrochemical recovery of tin and palladium from the activating solutions of the electroless plating of polymers potentiostatic operation, Sep Purif. Technol. 45 (2005) 183–191, https://doi.org/10.1016/j.seppur.2005.03.008.
[27] Q. Xia, Q. Song, Z. Xu, Electrorefining and electrodeposition for metal separation and purification from polymetallic concentrates after waste printed circuit board smelting, Waste Manag. 158 (2023) 146–152, https://doi.org/10.1016/j.wasman.2023.01.014.
[28] L. Hernández-Pérez, J. Carrillo-Abad, E.M. Ortega, V. Pérez-Herranz, M. T. Montañés, M.C. Martí-Calatayud, Voltammetric and electrodeposition study for the recovery of antimony from effluents generated in the copper electrorefining process, J. Environ. Chem. Eng. 11 (2023) 109139, https://doi.org/10.1016/J.JECE.2022.109139.
[29] L. Hernández-Pérez, J. Carrillo-Abad, V. Pérez-Herranz, M.T. Montañés, M. C. Martí-Calatayud, Effluents from the copper electrorefining as a secondary source of antimony: Role of mass transfer on the recovery by electrodeposition, Desalination 549 (2023) 116322, https://doi.org/10.1016/j.desal.2022.116322.
[30] F. Arroyo-Torralvo, A. Rodríguez-Almansa, I. Ruiz, I. González, G. Ríos, C. Fernández-Pereira, L.F. Vilches-Arenas, Optimizing operating conditions in an ion-exchange column treatment applied to the removal of Sb and Bi impurities from an electrolyte of a copper electro-refining plant, Hydrometallurgy 171 (2017) 285–297, https://doi.org/10.1016/j.hydromet.2017.06.009.
[31] P. Zimmermann, Ö. Tekinalp, S.B.B. Solberg, Ø. Wilhelmsen, L. Deng, O. S. Burheim, Limiting current density as a selectivity factor in electrodialysis of multi-ionic mixtures, Desalination 558 (2023), https://doi.org/10.1016/j.desal.2023.116613.
[32] F. Besse, C. Boulanger, J.M. Lecuire, Preparation of $Bi_{1-x}Sb_x$ films by electrodeposition, J. Appl. Electrochem 30 (2000) 385–392, https://doi.org/10.1023/A:1003990327662.
[33] J. Schoenleber, N. Stein, C. Boulanger, Influence of tartaric acid on diffusion coefficients of Bi^{III}, Sb^{III}, Te^{IV} in aqueous medium: application of electrodeposition of thermoelectric films, J. Electroanal. Chem. 724 (2014) 111–117, https://doi.org/10.1016/j.jelechem.2014.04.004.
[34] D.J. Suárez, Z. González, C. Blanco, M. Granda, R. Menéndez, R. Santamaría, Graphite felt modified with bismuth nanoparticles as negative electrode in a vanadium redox flow battery, ChemSusChem 7 (2014) 914–918, https://doi.org/10.1002/cssc.201301045.
[35] M.S. Martín-González, A.L. Prieto, R. Gronsky, T. Sands, A.M. Stacy, Insights into the electrodeposition of Bi_2Te_3, J. Electrochem Soc. 149 (2002) C546, https://doi.org/10.1149/1.1509459.
[36] M. Martín-González, A.L. Prieto, M.S. Knox, R. Gronsky, T. Sands, A.M. Stacy, Electrodeposition of $Bi_{1-x}Sb_x$ films and 200-nm wire arrays from a nonaqueous solvent, Chem. Mater. 15 (2003) 1676–1681, https://doi.org/10.1021/cm021027f.